

Original article

On the dose to a moving target while employing different IMRT delivery mechanisms

Eric D. Ehler^a, Benjamin E. Nelms^c, Wolfgang A. Tomé^{a,b,*}^aDepartment of Medical Physics, and ^bDepartment of Human Oncology, University of Wisconsin, Madison, WI, USA,
^cCanis Lupus LLC, St. Louis, MO, USA

Abstract

Background and purposes: To compare the temporal uniformity in dose delivered to a moving target for various intensity modulation radiotherapy (IMRT) modalities: solid intensity modulator (SIM), segmented multi-leaf collimator (SMLC), and dynamic multi-leaf collimator (DMLC).

Materials and methods: Two separate four-dimensional computed tomography data sets were obtained. Tumor motion kernels and motion envelopes were determined from composite positions of the tumor in various phases of the breathing cycle. Treatment plans were created for an unmodulated open field, SIM, SMLC, and DMLC. The motion envelope was treated as a static target volume. A robotic apparatus equipped with a diode array simulated the tumor motion in the plane of the beam's eye view (BEV). Radiation was delivered to the moving target over ten trials for each modality. The average coefficient of variation (CV) was determined for each beam angle.

Results: The CV ranged from 0.09% to 0.15%, 0.23% to 3.14%, 1.14% to 5.51%, and 3.83% to 8.25% for the unmodulated open field, SIM, SMLC, and DMLC modalities, respectively. With gating, the CV was 0.23% to 2.31%, 0.31% to 2.97%, and 0.7% to 4.67% for SIM, SMLC, and DMLC, respectively.

Conclusion: SIM consistently provided the most temporally uniform dose to the moving target while DMLC provided the least. The SMLC and DMLC CV improved with gated delivery.

© 2007 Elsevier Ireland Ltd. All rights reserved. Radiotherapy and Oncology xx (2007) xxx–xxx.

Keywords: 4D IMRT; Intrafraction motion; Gating; Gated IMRT delivery; Temporal dose uniformity

Radiotherapy is the main treatment course for unresectable non-small cell lung cancer (NSCLC). The ultimate goal of 4D-IMRT is to deliver dose accurately to a moving target so that the target volume receives the planned dose while keeping the dose to the adjacent normal tissue and critical structures as low as possible. Statically planned non-uniform dose distributions will cause parts of a moving target to receive a dose lower than the prescribed dose.

The intra-fractional motion of the patient anatomy with respect to the movement of the multi-leaf collimators (MLC) is commonly called the interplay effect. Yu et al. [11] showed that for a moving target, variation in photon fluence due to the interplay effect is averaged out after the delivery of a 30-fraction schedule. Subsequent simulations have reported the expected dose to a moving target to be independent of IMRT modality [3,5]. Bortfeld et al. [3,4] have stated that the main effect of target motion is blurring of the delivered dose distribution and that this effect is independent of delivery technique, i.e. that the average dose distribution resulting from this blurring effect is independent of delivery technique. However Bortfeld et al. [3] found that unlike the average dose distribution,

the variations around the average dose distribution do depend on the employed delivery technique. Using Monte Carlo simulation techniques and assuming a simple sinusoidal breathing motion, they showed that solid compensator-based IMRT delivery exhibits a smaller variation than does MLC based IMRT delivery. This study compares the variation of dose delivered to a moving target on a field-by-field basis using an unmodulated open field, solid intensity modulator (SIM), segmented multi-leaf collimator (SMLC), and dynamic multi-leaf collimator (DMLC) employing a specifically designed two dimensional multidetector robotic phantom that is able to trace out actual patient breathing patterns [9]. Gated IMRT delivery was investigated for the three different IMRT delivery techniques: SIM, SMLC, and DMLC.

Materials and methods

In order to commission SIM for use in this study, broad beam attenuation coefficients were determined using .decimal[®] (Sanford, FL) SIM calibration blocks. A 3-cm thick block of brass was attached to the tray of the Varian Clinac

600C/D equipped with a 120 leaf MLC. Readings were taken at a depth of 10 cm in a water equivalent material, SOLID WATER[®] (GAMMEX rmi[®], Middleton, WI), for various field sizes. The attenuation coefficients were used to determine the thickness required for the SIM modulators. Six megavolt X-rays were used for attenuation coefficient measurements and for the dose uniformity measurements.

4D-CT data (acquired using a double vacuum immobilization device combined with an abdominal pressure pillow for breathing restriction) from two lung tumor cases that had previously been treated using stereotactic body radiation therapy (SBRT), designated hereafter as SBRT1 and SBRT2, were used to derive the actual patient specific breathing trajectory of each of the tumors. The breathing trajectories were used to automatically generate a motion envelope [12]. SBRT1 had a greater tumor excursion in the cephalad–caudal direction than SBRT2 (2 cm versus 1.4 cm, respectively) and SBRT1 had a greater tumor speed in the motion envelope as well. The average periods of motion as measured during 4D-CT acquisition for SBRT1 and SBRT2 were 4.6 and 4.0 s, respectively. The motion envelope was treated as a static target volume and treatment plans were generated for each of the two lung cancer cases. Of the nine fields per treatment plan, the two fields with the highest modulation factor were used in this experiment. In total, four fields were used in this experiment (two fields per patient).

In order to study the effect of tumor motion due to respiration within the motion envelope during the delivery of a particular treatment field, a 4D motion kernel was generated for each of the beam angles considered. The motion kernel is defined here as the projection of the tumor motion perpendicular to the beam's eye view (BEV). Each breathing phase obtained from the 4D-CT was considered to be equidistant in time. The time interval between phases was determined by dividing the breathing motion period by the number of intervals between breathing phases. The coordinates (x, y, z) (t) were determined from the 4D-CT for the associated breathing phases.

A robotic apparatus and associated software was used to simulate tumor motion (cf. Figure EA-6 and Videos 1 and 2 in the Electronic appendix) [9]. The breathing motion was simulated with respect to the BEV in two spatial dimensions perpendicular to the beam using the motion kernel derived from the 4D-CT data. The apparatus utilizes two motors that drive the tabletop of the apparatus in the two spatial dimensions orthogonal to the treatment beam. Since the apparatus can only move orthogonal to the treatment beam, motion in the direction of the treatment beam could not be simulated. Deformation associated with breathing was not considered.

Delivered dose distributions were measured using a MapCHECK[™] diode array (Sun Nuclear, Melbourne, FL) that was attached to the tabletop of the breathing motion apparatus along with three inches of solid water placed on top of the diode array. The spacing between diodes in the array was 7.07 mm. Tumor mimicking diodes were determined based on the BEV projection of the expiration phase gross tumor volume (GTV) generated by the Pinnacle³ 7.9v treatment planning system (Philips Medical, Madison, WI). The appropriate BEV projection of the GTV shape was then placed

on the MapCHECK[™], which displays the location of the diodes as well as the coordinate system used to locate individual diodes by the MapCHECK[™] software. The diodes within the BEV projection of the GTV shape were then recorded for each beam angle considered. For SBRT1, seven diodes were designated as tumor mimicking for both treatment fields investigated, while for SBRT2, 15 diodes were used as tumor mimicking for both treatment fields. The breathing motion apparatus was then set in motion and it traced out the simulated breathing pattern corresponding to the BEV of the treatment field that was to be delivered. While the apparatus repeatedly cycled through the motion kernel, radiation was delivered starting at a random breathing phase. This procedure was repeated 10 times for the unmodulated open field delivery and each of the three IMRT delivery techniques, SIM, SMLC, and DMLC, and for each of the fields investigated.

For the gated study, only the 50% phase (full expiration) of the 4D-CT was used in treatment planning. Gating was possible by monitoring a marker block extending from the rear of the MapCHECK[™] array using the Real-Time Position Management (RPM[™]) system (Varian, Palo Alto, CA). In order to utilize the RPM-system already in place, the horizontal motion of the 2D robotic MapCHECK[™] apparatus was translated to vertical motion by placing a ramp behind the apparatus (cf. Video 3 in the Electronic appendix) [9]. When this system is used clinically for a patient, the marker block is placed on the patient in close proximity to the tumor location in the cephalad–caudal direction during the acquisition of the 4D-CT to ensure that the breathing amplitude detected by tracking the marker block is correlated to the respiratory motion of the tumor. In this experiment, the correlation between tumor respiratory motion and the breathing amplitude detected by the RPM system was achieved by directly coupling the marker to the 2D robotic MapCHECK[™] apparatus. Radiation was delivered at the exhalation phase because it has been shown to be the most reproducible phase [1,10]. The duty cycle was set to 30% for the gated study. The position of the marker box was tracked by the RPM-system during the actual treatment delivery (cf. Video 4 in the Electronic appendix).

Fluence maps acquired from the treatment planning system were convolved with the motion kernel for each field (cf. Figs. 1 and 2). The fluence maps had a resolution of 2.5 mm. The convolved fluence maps along with the data in Table 1 were used to determine the differences in the static dose distributions between the IMRT modalities.

Data for each individual tumor mimicking diode were analyzed as a set over the 10 trials for each of the following delivery techniques: unmodulated open field, SIM, SMLC, and DMLC. For both SLMC and DMLC delivery, the motion of the MLC leaves was perpendicular to the cephalad–caudal breathing motion of the target. In order to keep beam delivery times within reason, a dose of 2 Gy per fraction was prescribed to the isocenter. For a single trial, the MapCHECK[™] data file reported the raw data and the associated correction factors, calibration factors, and the absolute dose for each diode. In the data file, the diodes were designated with the same coordinate system displayed on the face of the MapCHECK[™] unit, which was previously used to specify the tumor mimicking diodes. This made it possible

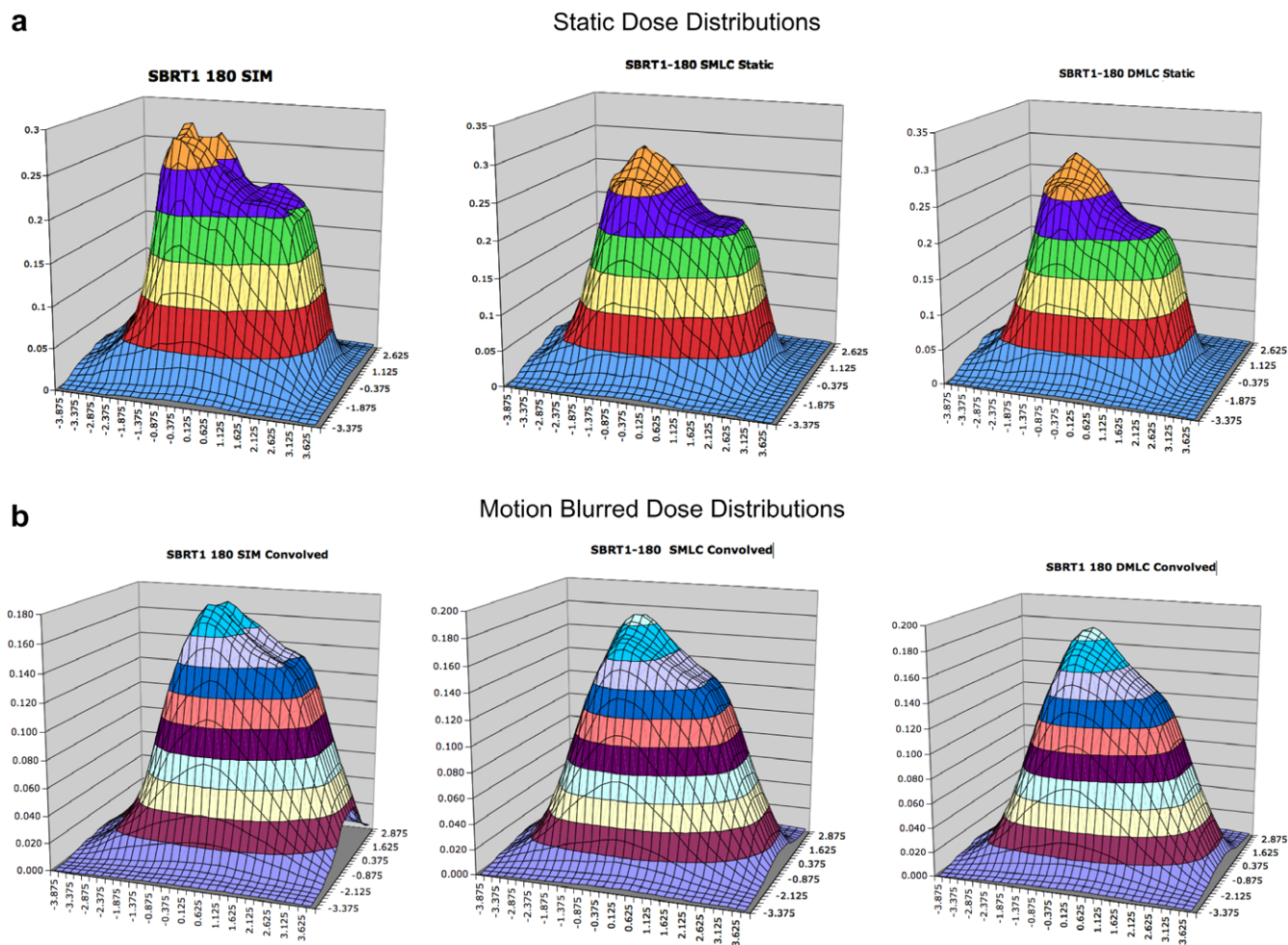


Fig. 1. Underlying static and motion blurred IMRT dose distributions for beam SBRT1-180. (a) Shows from left to right the static IMRT dose distribution for SIM, SMLC, and DMLC, respectively. While (b) shows those corresponding to the blurred IMRT dose distribution obtained by convolving the static dose distribution with the probability density function corresponding to the motion kernel of patient 1.

to determine what data were associated with the tumor mimicking diodes. The absolute doses for the tumor mimicking diodes were imported into a computer program for data analysis.

Results

The coefficient of variation (CV) is defined as:

$$CV = \frac{\sigma}{\bar{d}} \times 100\%$$

where σ is the standard deviation in the readings for a single diode over the 10 trials. For an unmodulated open field, \bar{d} is the average reading for a single diode over 10 trials. For an IMRT delivered field, \bar{d} is a common average dose for each diode detector that is the arithmetic average of the average doses measured for the SIM, SMLC, and DMLC delivery (see Discussion below).

The average CV was determined for all tumor mimicking diodes representing the GTV for a particular treatment field. The CV is meant to quantify the variation in dose to

each of the tumor mimicking diodes. A smaller CV indicates a more temporally uniform dose to the “tumor” over multiple fractions for the IMRT modality considered. Bortfeld and colleagues [3,4] have shown using general arguments that, for a given static dose distribution, the average dose of the motion blurred dose distribution is independent of the IMRT delivery technique. The experimentally determined average doses of each diode detector, measured using actual patient breathing traces, therefore should be independent of the IMRT delivery technique. To test this, a two-sided t -test with unequal variance was performed for each of the diode detectors comparing the average doses measured for each IMRT delivery modality. These t -tests showed that for some diode detectors the average dose differences between different IMRT modalities reach statistical significance. This indicates that these differences are not entirely due to the random measurement process, but are also due to differences in the underlying static IMRT dose distributions that are not smoothed out by the blurring of the dose distribution (cf. Figs. 1 and 2, Table 1 and for the complete data cf. Table EA-1 a and b in the Electronic appendix). As seen in Table 1, the average dose measured by the same

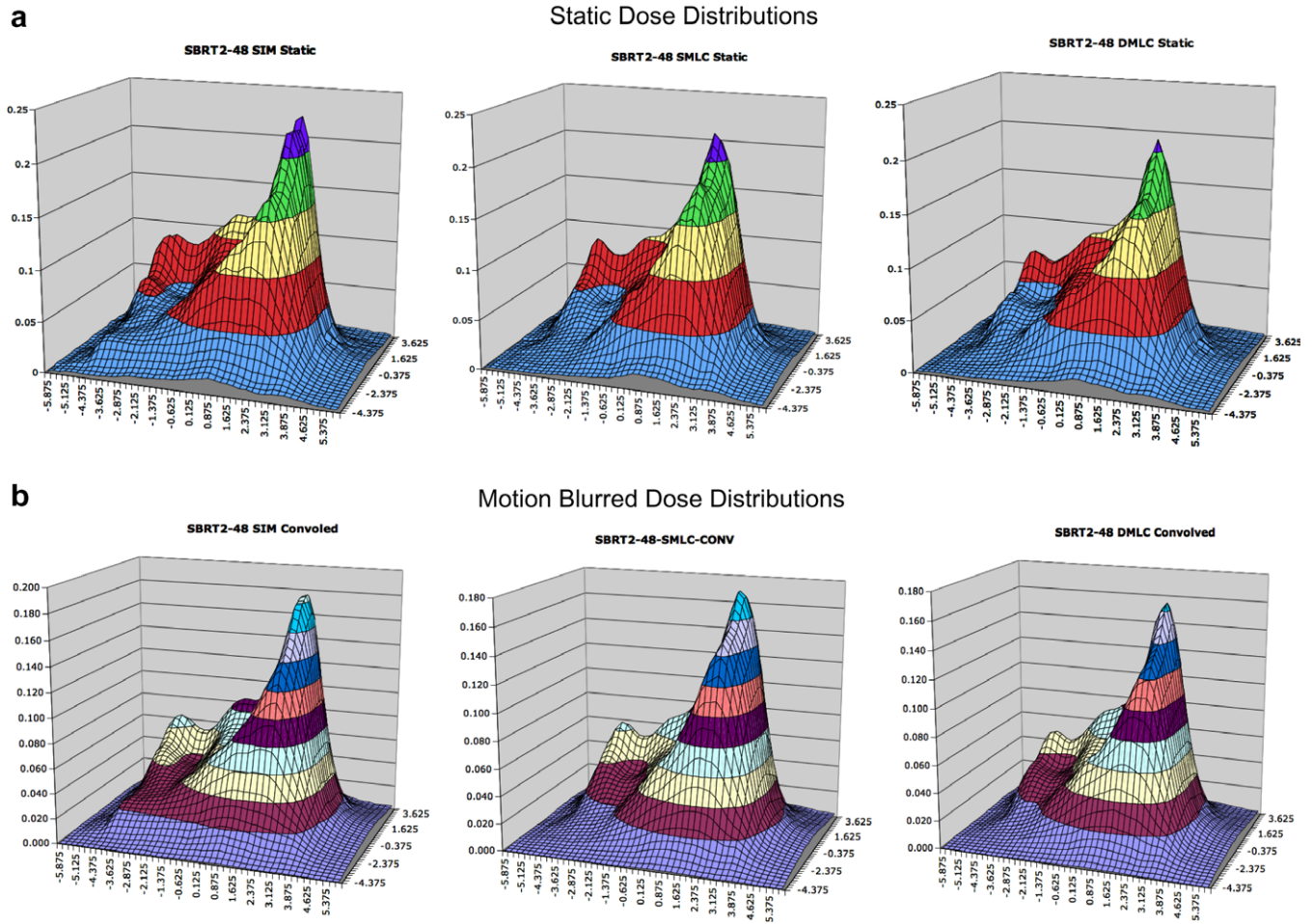


Fig. 2. Underlying static and motion blurred IMRT dose distributions for beam SBRT2-48. (a) Shows from left to right the static IMRT dose distribution for SIM, SMLC, and DMLC, respectively. While (b) shows those corresponding to the blurred IMRT dose distribution obtained by convolving the static dose distribution with the probability density function corresponding to the motion kernel of patient 2.

Table 1

Comparison of average doses measured using tumor mimicking diodes for the non-gated and gated IMRT delivery modalities SIM, SMLC, and SBRT using a two-sided t -test assuming unequal variance

	SBRT1-180			SBRT1-279		
	SIM-SMLC % $\bar{\Delta} \pm \sigma$	SMLC-DMLC % $\bar{\Delta} \pm \sigma$	SIM-DMLC % $\bar{\Delta} \pm \sigma$	SIM-SMLC % $\bar{\Delta} \pm \sigma$	SMLC-DMLC % $\bar{\Delta} \pm \sigma$	SIM-DMLC % $\bar{\Delta} \pm \sigma$
<i>Ungated</i>						
Significant	4.09% \pm 2.37%	5.54% \pm 2.64%	6.83% \pm 1.35%	2.88% \pm 1.57%	2.49%	4.01%
Non-significant	0.74% \pm 0.19%	2.49% \pm 1.62%	0.76% \pm 0.50%	0.22% \pm 0.12%	0.94% \pm 0.80%	1.29% \pm 0.91%
<i>Gated</i>						
Significant	6.04% \pm 5.71%	15.11% \pm 5.95%	18.42% \pm 9.72%	6.04% \pm 5.71%	15.11% \pm 5.95%	18.42% \pm 9.72%
Non-significant	0.28%	N/A	N/A	0.28%	N/A	N/A
	SBRT2-048			SBRT2-213		
	SIM-SMLC % $\bar{\Delta} \pm \sigma$	SMLC-DMLC % $\bar{\Delta} \pm \sigma$	SIM-DMLC % $\bar{\Delta} \pm \sigma$	SIM-SMLC % $\bar{\Delta} \pm \sigma$	SMLC-DMLC % $\bar{\Delta} \pm \sigma$	SIM-DMLC % $\bar{\Delta} \pm \sigma$
<i>Ungated</i>						
Significant	8.88% \pm 4.63%	10.79% \pm 4.70%	10.79% \pm 5.48%	6.94% \pm 4.78%	9.24% \pm 4.79%	8.78% \pm 5.90%
Non-Significant	5.03% \pm 4.79%	5.72% \pm 2.96%	2.68% \pm 2.58%	1.08% \pm 0.86%	1.98% \pm 0.36%	3.17% \pm 2.35%
<i>Gated</i>						
Significant	9.79% \pm 7.02%	20.64% \pm 8.79%	26.49% \pm 12.08%	45.10% \pm 10.97%	6.16% \pm 3.32%	47.92% \pm 13.13%
Non-Significant	0.78% \pm 0.61%	0.29%	N/A	N/A	2.56% \pm 2.24%	N/A

The symbol “% $\bar{\Delta} \pm \sigma$ ” denotes the average percent change together with its associated standard deviation if applicable between the two IMRT modalities listed.

diode detector for a given non-gated delivered IMRT field using SIM, SMLC, or DMLC can differ by up to 6.83% for the IMRT treatment fields with the lower degree of modulation (SBRT1-180° & - 279°) and by up to 10.79% for the IMRT

treatment fields with a high degree of modulation (SBRT2-48° & - 213°). For the gated delivery, the differences in diode readings are even more pronounced since the static dose distributions are no longer blurred due to motion and

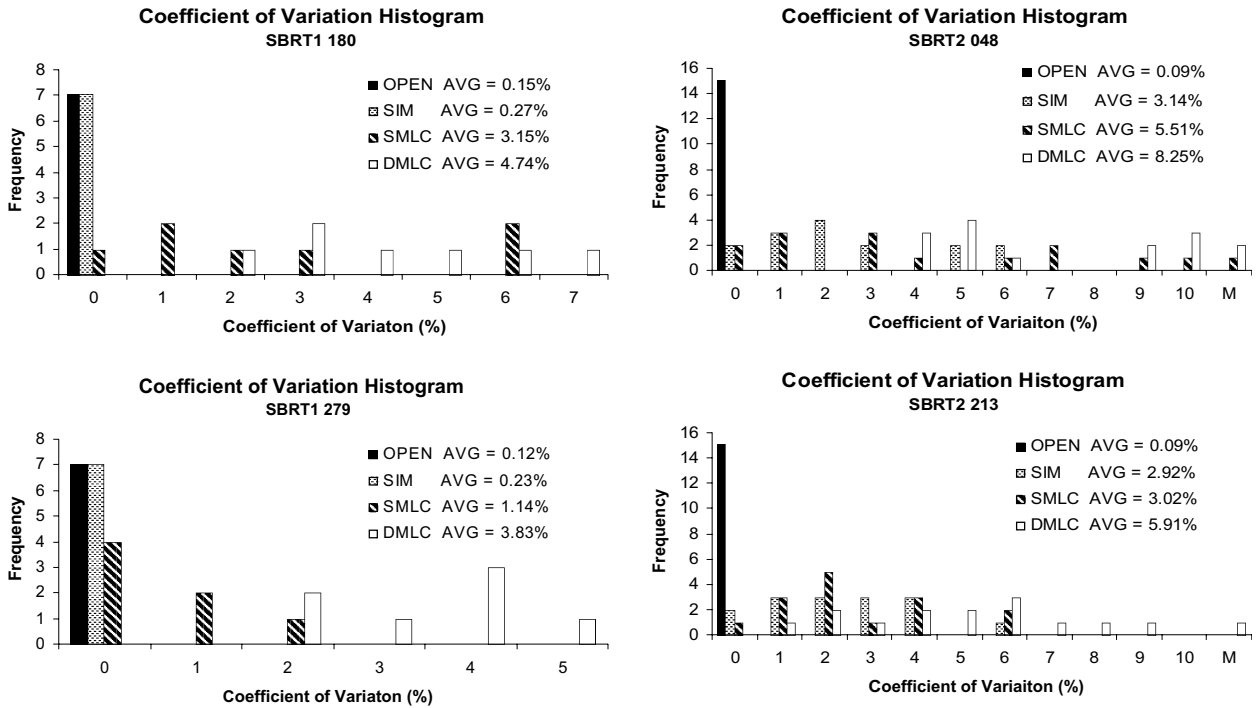


Fig. 3. Non-gated CV histogram for all modalities of SBRT1 at 180° and 279° beam angles and SBRT2 at 48° and 213° beam angles. Average CV values for each modality are listed as "AVG = " on the histograms. On the x-axis "M" indicates diodes with CV values greater than 10%.

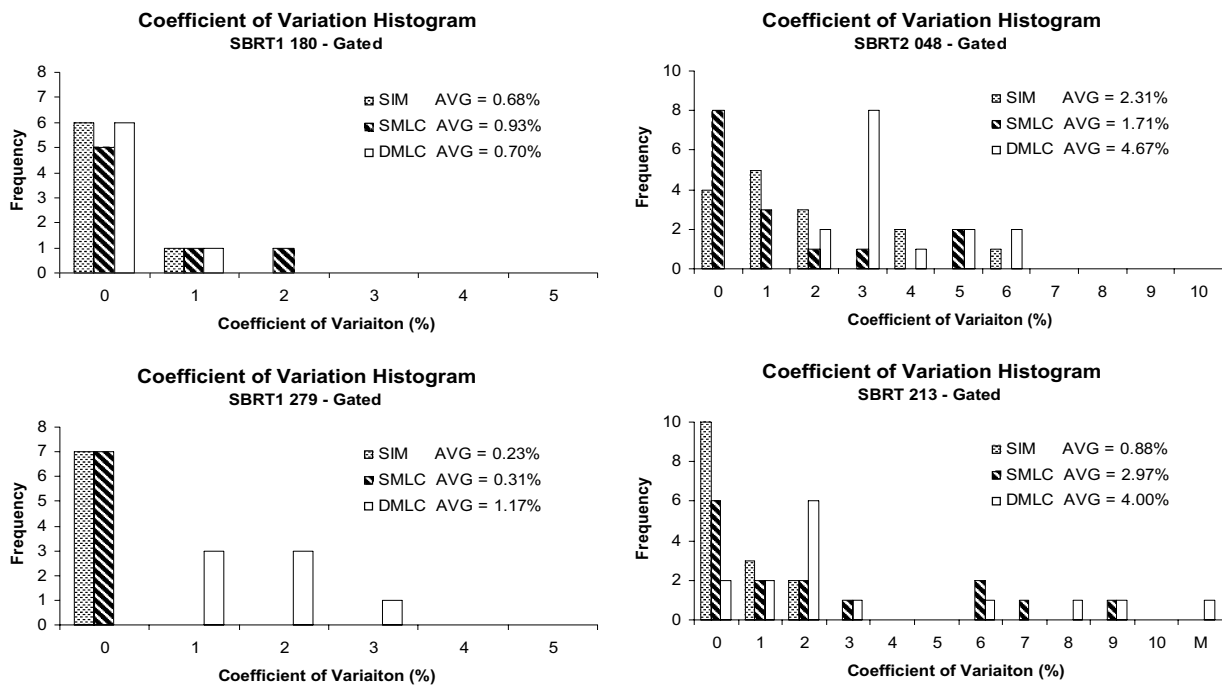


Fig. 4. Gated CV histogram for all modalities of SBRT1 at 180° and 279° beam angles and SBRT2 at 48° and 213° beam angles. Average CV values for each modality are listed as "AVG = " on the histograms.

can be as large as 18.42% and 47.92% for lower modulated and higher modulated fields, respectively. Therefore, in order to compare the CV for the three different IMRT delivery modalities, a common average dose for each diode detector that is the arithmetic average of the average doses measured for the SIM, SMLC, and DMLC delivery was used. Hence, using these common average doses the CV can then be used to describe the temporal uniformity for a given IMRT modality.

For analysis, the CV values of the different tumor mimicking diodes were binned and arranged in a histogram of Frequency vs. CV plot. These histograms illustrate the distribution of the dose variation to the tumor mimicking diodes.

Fig. 3 shows the data for the non-gated delivery of the fields SBRT1-180° and SBRT1-279° as well as the fields SBRT2-48° and SBRT2-213° for the four delivery techniques: unmodulated open field, SIM, SMLC, and DMLC. In Fig. 4, the histogram plots of Frequency vs. CV for gated delivery of the same fields as in Fig. 3 are shown for the three IMRT delivery techniques (SIM, SMLC, and DMLC). Note that the scale of the Frequency-axis does not stay constant for the SBRT2 data between the gated and non-gated data. A CV of ‘‘0’’ indicates the CV was between 0% and 1% and the frequency indicates the number of diodes with the associated CV value. The average CV for all diodes is also shown in the CV histogram for each of the studied delivery techniques. For open field delivery the CV ranged from 0.09% to 0.15%, while for SIM it ranged from 0.23% to 3.14%, for SMLC delivery it ranged from 1.14% to 5.51%, and lastly for DMLC delivery it ranged from 3.83% to 8.25%. These results indicate that SIM delivers the most temporally uniform IMRT dose distribution to a moving target, followed by SMLC, while DMLC delivers the least temporally uniform dose distribution to a moving target. With gating, the CV ranges improved and were found to be 0.23–2.31%, 0.31–2.97%, and 0.7–4.67% for SIM, SMLC, and DMLC, respectively.

Delivery times comparing non-gated and gated delivery are shown in Table EA-2 in the Electronic appendix. One beam angle for each patient was used to compare the delivery times. The SMLC deliveries had 5 and 10 segments for SBRT1-180° and SBRT2-048°, respectively.

Discussion

From Fig. 3, one can see that of the three non-gated IMRT delivery methods (SIM, SMLC, and DMLC) SIM consistently provided a more temporally uniform dose to the tumor over 10 trials for a non-gated delivery. For the two SBRT1 treatment fields, the average CV of the SIM deliveries is roughly twice that of the control cases (the open unmodulated fields). The average CV of the best performing MLC delivery was an order of magnitude greater than that of the unmodulated open field.

Bortfeld et al. [3,4] found a variation of the order of 0.5% for SIM and 1.0–2.0% for MLC delivery of a single field using Monte Carlo simulation, which agrees with what we found for the non-gated SBRT1 treatment fields. A theoretical tumor with a 1-cm displacement and a period of 4.1 s was used

in the Monte Carlo simulation [3]. The above variations have been estimated for the simulated delivery of 30 treatment fractions over 1000 trials. For the SBRT2 treatment fields, a variation larger than that predicted by Bortfeld et al. [3] was found, which is likely due to the high degree of modulation in the SBRT2 treatment fields (see Figure EA-5 in the Electronic appendix). A higher degree of modulation can cause a moving target to receive a larger dose variation due to the interplay effect. Both tumors in this study were located near the diaphragm resulting in displacements of 2 cm for SBRT1 and 1.4 cm for SBRT2 in the cephalad–caudal axis, which is greater than the 1 cm displacement considered by Bortfeld et al. [3]. Larger displacements can contribute also to a larger dose variation for MLC delivered IMRT. The SBRT1 study, which has the lower degree of modulation but also has the largest displacement, generally agreed with the data presented in Bortfeld et al. [3]. This suggests that the tumor displacement is not the dominant source of the dose variation in the present case.

SBRT2 has a greater degree of modulation than SBRT1 (see Figure EA-5 in the Electronic appendix). For all but one case, the average CV for all IMRT modalities increased from SBRT1 to SBRT2 (cf. Figs. 3 and 4). For the SMLC delivery of the SBRT1-180° field (five intensity levels) and the SBRT2-213° field (seven intensity levels), there is no significant difference in the average CV between the two fields, even though SBRT2-213° has a higher level of modulation. The rest of the data suggests that the temporal dose uniformity can decrease with an increasing degree of modulation in the treatment beam.

From the data for SBRT1 (cf. Figs. 3 and 4), it can be seen that the non-gated SIM performed as well as the gated MLC deliveries. It can also be seen from the data that SBRT2 had a significantly lower variation when delivered in gated mode compared to non-gated. This suggests that for treatment plans with high modulation, gated delivery could provide the best inter-fractional temporal uniformity for the total delivered dose distributions, i.e. minimizing the interplay effect for all fields. For lower degrees of modulation, a non-gated SIM delivery could provide the same inter-fractional temporal dose uniformity as a gated MLC delivery. For a discussion on how to decide what delivery technique is appropriate see Nelms and Tomé [9] Of course, for cases where using a SIM is not practical, SMLC could be a good compromise.

SMLC and DMLC showed significant improvement for gated delivery over that of non-gated delivery (cf. Figs. 3 and 4). Table 2 shows the percent ratio improvement in CV from non-gated to gated delivery. Furthermore, one can see from Figs. 3 and 4 that DMLC consistently delivers the least temporally uniform dose to the tumor over many trials. The only case in which DMLC did not provide the least temporally uniform dose is the gated delivery of the SBRT1-180° field. For this beam there is no significant difference between all three IMRT delivery techniques (cf. Fig. 4). This is, of course, expected since gating minimizes the interplay effect between target motion and MLC motion. These results, however, do not correlate with a previous study which found that a sliding window technique (DMLC) delivers a more temporally uniform dose than step and shoot (SMLC) for seven out of 10 treatment fields [7]. This study involved

Table 2
Percent ratio of non-gated CV to gated CV

	SBRT1-180	SBRT1-279	SBRT2-048	SBRT2-213
<i>Percent ratio improvement in CV from non-gated to gated delivery</i>				
SIM	None	None	135.93%	331.82%
SMLC	338.71%	367.74%	322.22%	101.68%
DMLC	677.14%	327.35%	176.66%	147.75%

There was no improvement for the SIM delivered fields for SBRT1.

two patient plans (five fields per patient) with 30 fractions to a tumor with a 4-s period and 2 cm displacement and a dose rate of 300 MU/min. In the study by Jiang et al. [7], step and shoot IMRT was performed with 10 and 20 intensity levels while the treatment plans in our study called for 5, 3, 10, and 7 intensity levels for the SBRT1-180°, SBRT1-279°, SBRT2-048°, and SBRT2-213° fields, respectively. It is also important to note that dose measurements in the study by Jiang et al. [7] were made with a single 0.6-cc farmer chamber while this study used a multidetector diode array. For each field investigated, diode detectors can be found for which the observation made by Jiang and colleagues [7] is true. However, these diodes represent a distinct minority of all diode detectors.

Many studies on the variation of dose to a moving target [2,3,5,8,11] have assumed a treatment schedule of 30 fractions of 2 Gy per fraction. A relatively new technique for treating some thoracic tumors is SBRT, which utilizes extreme hypofractionation. At our institution a schedule consisting of five fractions of 12 Gy [6] is used. The modeling study by Bortfeld et al. [3] has illustrated the fact that there is a significant difference in the dose variation between five and 30 fractions. The dose distribution was found to still have a Gaussian form at only five fractions but with an increased standard deviation, indicating an increase in variation about the average dose distribution. It can be seen from the data for SBRT2 that a large variation in dose is quite possible when the number of fractions is less than 30, specifically in this experiment 10. However, with larger doses per fraction, the variation due to the interplay effect should decrease due to the longer treatment time for each field since the MLC clustering scheme is independent of the dose per fraction being delivered. If the delivery time for each field is significantly lengthened, in this case by a factor of 6, the number of breathing periods the tumor undergoes for each field would also increase by a factor of 6. Thus for any IMRT field, the initial tumor position will have less of an effect on the dose to the tumor for a given fraction since the tumor will undergo many more breathing cycles.

Conclusions

For non-gated 4D-IMRT, SIM consistently provided the most temporally uniform dose to a tumor over many trials while DMLC consistently provided the least temporally uniform dose. With gating, SMLC and DMLC showed significant improvement. DMLC showed the greatest improvement with

gating and therefore should be delivered in gated mode. For the case with the largest motion displacement and lower modulation, SBRT1, non-gated SIM performed as well as gated MLC delivery over the 10 trials.

Appendix A. Supplementary data

Supplementary data associated with this article can be found, in the online version, at [doi:10.1016/j.radonc.2007.02.007](https://doi.org/10.1016/j.radonc.2007.02.007).

* Corresponding author. Wolfgang A. Tomé, Department of Human Oncology, School of Medicine and Public Health, University of Wisconsin, K4/344 CSC, 600 Highland Avenue, Madison, WI 53792, USA. E-mail address: tome@humonc.wisc.edu

Received 24 October 2006; received in revised form 26 January 2007; accepted 13 February 2007

References

- [1] Baiter JM, Lam KL, McGinn CJ, Lawrence TS, Ten Haken RK. Improvement of CT-based treatment-planning models of abdominal targets using static exhale imaging. *Int J Radiat Oncol Biol Phys* 1998;41:939–43.
- [2] Berbeco RI, Pope CJ, Jiang SB. Measurement of the interplay effect in lung IMRT treatment using EDR2 films. *J Appl Clin Med Phys* 2006;7:33–41.
- [3] Bortfeld T, Jokivarsi K, Goitein M, et al. Effects of intra-fraction motion on IMRT dose delivery: statistical analysis and simulation. *Phys Med Biol* 2002;47:2203–20.
- [4] Bortfeld T, Jiang SB, Rietzel E. Effects of motion on the total dose distribution. *Sem Rad Oncol* 2004;14:41–51.
- [5] Chui CS, Yorke E, Hong L. The effects of intra-fraction organ motion on the delivery of intensity-modulated field with a multileaf collimator. *Med Phys* 2003;30:1736–46.
- [6] Hodge W, Tomé WA, Jaradat HA, et al. Feasibility report of image guided stereotactic body radiotherapy (IG-SBRT) with tomotherapy for early stage medically inoperable lung cancer using extreme hypofractionation. *Acta Oncol* 2006;45:890–6.
- [7] Jiang SB, Pope C, Al Jarrah KM, Kung JH, Bortfeld T, Chen GTY. An experimental investigation on intra-fractional organ motion effects in lung IMRT treatments. *Phys Med Biol* 2003;48:1773–84.
- [8] Kissick MW, Boswell SA, Jeraj R, Mackie TR. Confirmation, refinement, and extension of a study in intrafraction motion interplay with sliding jaw motion. *Med Phys* 2005;32:2346–50.

- [9] Nelms B, Tomé WA. A 4D IMRT QA device. *Med Phys* 2006;33:2247.
- [10] Seppenwoolde YM, Shirato H, Kitamura K, et al. Precise and real-time measurement of 3D tumor motion in lung due to breathing and heartbeat, measured during radiotherapy. *Int J Radiat Oncol Biol Phys* 2002;53:822–34.
- [11] Yu CX, Jaffray DJ, Wong JW. The Effects of intra-fraction motion on the delivery of dynamic intensity modulation. *Phys Med Biol* 1998;43:91–104.
- [12] Zhang T, Orton NP, Tomé WA. On the automated definition of mobile target volumes from 4D-CT images for stereotactic body radiotherapy. *Med Phys* 2005;32:3493–502.